· Article · Advances in Polar Science
doi: 10.13679/j.advps.2020.0039 June 2021 Vol. 32 No. 2: 96-104

Factors contributing to rapid decline of Arctic sea ice in autumn

LI Shuyao[1,2], CUI Hongyan[1,2,3*], XU Junli[1,2], GONG Xiang[1,2], QIAO Fangli[3,4], YANG Yanzhao[1,4], WANG Ping[1], HAN Yuqun[1] & SHAN Feng[4]

[1] College of Mathematics and Physics, Qingdao University of Science and Technology, Qingdao 266061, China;
[2] Research Institute for Mathematics and Interdisciplinary Sciences, Qingdao University of Science and Technology, Qingdao 266061, China;
[3] Laboratory for Regional Oceanography and Numerical Modeling, Qingdao National Laboratory for Marine Science and Technology, Qingdao 266061, China;
[4] The First Institute of Oceanography, Ministry of Natural Resources, Qingdao 266061, China

Received 28 December 2020; accepted 11 June 2021; published online 30 June 2021

Abstract Autumn Arctic sea ice has been declining since the beginning of the era of satellite sea ice observations. In this study, we examined the factors contributing to the decline of autumn sea ice concentration. From the Beaufort Sea to the Barents Sea, autumn sea ice concentration has decreased considerably between 1982 and 2020, and the rates of decline were the highest around the Beaufort Sea. We calculated the correlation coefficients between sea ice extent (SIE) anomalies and anomalies of sea surface temperature (SST), surface air temperature (SAT) and specific humidity (SH). Among these coefficients, the largest absolute value was found in the coefficient between SIE and SAT anomalies for August to October, which has a value of −0.9446. The second largest absolute value was found in the coefficient between SIE and SH anomalies for September to November, which has a value of −0.9436. Among the correlation coefficients between SIE and SST anomalies, the largest absolute value was found in the coefficient for August to October, which has a value of −0.9410. We conducted empirical orthogonal function (EOF) analyses of sea ice, SST, SAT, SH, sea level pressure (SLP) and the wind field for the months where the absolute values of the correlation coefficient were the largest. The first EOFs of SST, SAT and SH account for 39.07%, 63.54% and 47.60% of the total variances, respectively, and are mainly concentrated in the area between the Beaufort Sea and the East Siberian Sea. The corresponding principal component time series also indicate positive trends. The first EOF of SLP explains 41.57% of the total variance. It is mostly negative in the central Arctic. Over the Beaufort, Chukchi and East Siberian seas, the zonal wind weakened while the meridional wind strengthened. Results from the correlation and EOF analyses further verified the effects of the ice–temperature, ice–SH and ice–SLP feedback mechanisms in the Arctic. These mechanisms accelerate melting and decrease the rate of formation of sea ice. In addition, stronger meridional winds favor the flow of warm air from lower latitudes towards the polar region, further promoting Arctic sea ice decline.

Keywords **Arctic sea ice, rapid decline, empirical orthogonal function, feedback mechanisms**

Citation: Li S Y, Cui H Y, Xu J L, et al. Factors contributing to rapid decline of Arctic sea ice in autumn. Adv Polar Sci, 2021, 32(2): 96-104, doi: 10.13679/j.advps.2020.0039

1 Introduction

Monthly Arctic sea ice extent (SIE) has been decreasing since 1979 for all months of the year and the long-term decline is more pronounced over the autumn months (September, October, November) (Perovich et al., 2020). The increase in melt season length (Belchansky et al., 2004; Gui et al., 2019) and the rapid decline of SIE (Comiso et al., 2008; Wu et al., 2012) are both related to Arctic warming

* Corresponding author, ORCID: 0000-0003-4221-9417, E-mail: cuihy@qust.edu.cn

(Stroeve et al., 2014; Lind et al., 2018). The rate of Arctic warming is twice the average global rate of warming (Cohen et al., 2014; Ballinger et al., 2020; Timmermans and Labe, 2020), and is referred to as Arctic amplification (Ding et al., 2017).

Arctic sea ice decline is a result of various processes, including changes in atmospheric circulation (Ogi and Rigor, 2013; Serreze and Stroeve, 2015), oceanic circulation (Ogi et al., 2008) and cloud cover (Lindsay et al., 2008; Letterly et al., 2016; Huang et al., 2019). Ding et al. (2017) indicated that trends in summertime atmospheric circulation may have contributed as much as 60% to the September SIE decline since 1979. This is because the troposphere over Greenland and the Arctic Ocean has a barotropic structure, and a stronger anticyclonic circulation has made the lower troposphere warmer and wetter, increasing the downward longwave radiation over the ice. Ogi and Rigor (2013) demonstrated that the winter westerly jet over the Beaufort Sea has contributed to accelerated decreases in the sea ice cover to the east of Europe and north of Alaska. The interannual variation of September SIE in the Arctic Ocean is associated with summer sea level pressure (SLP) and surface air temperature (SAT) at high northern latitudes, and the years with low September SIE are characterized by anticyclonic circulation anomalies (Ogi and Wallace, 2007).

The variations in sea ice volume can be explained reasonably well by the anomalous exchanges of sea ice, air, and water between the North Atlantic and the Arctic (Goosse et al., 2004). A strong jet or high jet latitude increases the sea ice fraction over the Labrador Sea and decreases the sea ice fraction along the eastern side of Greenland (Ma et al., 2020). Lindsay et al. (2008) investigated the connection between changes in sea ice and cloud cover over the Arctic seas during autumn. They showed that the retreat of sea ice was associated with a decrease in cloud cover in the lower layer and an increase in cloud cover in the middle layer. Although these studies have identified several factors contributing to the general observed decline in sea ice, factors contributing to sea ice decline at specific times of the year, such as the month of September, have yet to be investigated.

Ogi et al. (2016) reported that the interannual variability of September SIE since 2007 is related to the surface temperatures of the Beaufort Sea, the Chukchi Sea and the East Siberian Sea. The Arctic Oscillation (AO) is the leading empirical orthogonal function (EOF) of the wintertime SLP, and is a large scale mode of climate variability (Thompson and Wallace, 1998). Changes in the AO have led to increased cyclonic activities in the Arctic region, accelerating sea ice decline (Rigor et al., 2002; Nakamura et al., 2015). The melting and freezing of Arctic sea ice are significantly correlated with the seasonal strength of the AO (Belchansky et al., 2004; Yang et al., 2016). Nakamura et al. (2015) showed that the recent reduction in November SIE has led to more negative phases of AO and North Atlantic Oscillation (NAO) in early and late winter. Moreover, positive AO and positive NAO contribute to reduction in winter sea ice, while the positive Pacific/North American Pattern (PNA) contributes to reduction in summer sea ice (Zhang et al., 2020). Sea ice thickness and net surface longwave radiation are also significant drivers of rapid sea ice decline (Markus et al., 2009; Urrego‐Blanco et al., 2019). Kwok (2018) summarized the large-scale changes in ice thickness, ice volume and multiyear ice coverage and concluded that the Arctic ice cover has thinned. Urrego‐Blanco et al. (2019) reported a positive correlation between SIE and net surface longwave radiation in the melting season and a negative correlation in the freezing season. Studies have also used EOF analysis to investigate atmospheric influences on Arctic sea ice (Liang et al., 2020; Platov et al., 2020). To improve our understanding of Arctic sea ice decline, this study uses EOF analysis to examine the relationships between Arctic sea ice and different dynamic and thermodynamic variables over the periods of July to September, August to October and September to November.

By examining lower atmospheric and upper oceanic circulations in the Arctic region in autumn, we aim to identify factors contributing to the rapid decline in Arctic sea ice in autumn. In Section 2, we present our methods and data sources. In Section 3, we describe the long-term trends of Arctic sea ice in autumn, and investigate the influences of sea surface temperature (SST), SAT, specific humidity (SH), SLP and wind fields on SIE decline in autumn. Conclusions and discussion are presented in Section 4.

2 Data and methods

We used National Oceanic and Atmospheric Administration (NOAA) optimum interpolation (OI) SST Version 2 (V2) monthly mean SST and sea ice concentration (SIC) data, which have spatial resolutions of 1°×1°, and the temporal coverage is from December 1981 to April 2021. Monthly SIE data were obtained from the National Snow and Ice Data Center (NSIDC) for the period November 1978 to April 2021 (Fetterer, 2017). Surface air temperature, SLP, surface winds and SH were obtained from the National Center for Atmospheric Research/ National Center for Atmospheric Research (NCEP/NCAR) Reanalysis 1 project. The data have spatial resolutions of 2.5°×2.5° and cover the time period from January 1948 to April 2021. All the selected variables are distributed from 60°N to 90°N and covered the period from 1982 to 2020. The period analyzed in this paper was chosen for when all data products were available.

Empirical orthogonal function analysis is used in meteorological and climate studies to analyze the spatial and temporal variability of single geophysical fields (Thompson and Wallace, 1998). It is also known as space–time decomposition, whereby $X = EOF_{m\times m} \times PC_{m\times n}$; m refers to the location in space, n indicates the length of the time

series, EOF corresponds to the spatial patterns of variability, and PC is the principal component (PC) and corresponds to the temporal patterns of variability. The EOFs are also known as the spatial modes. They reflect the spatial distribution of the factor field, and their values represent the degree of variability. The PC is also known as the time coefficient, and reflects the weight change of the corresponding spatial mode with time.

3 Results

Figure 1 shows the spatial distribution of autumn SIC anomalies. Over most parts of the Arctic, sea ice in the autumn retreated considerably between 1982 and 2020. The decline was mainly concentrated in the Beaufort Sea, the Chukchi Sea, the East Siberian Sea, the Laptev Sea, the Kara Sea and around the Barents Sea, and was the most pronounced in the Beaufort and Chukchi seas (Figure 1a and 1b). The decline of Arctic sea ice in autumn is related to many factors. Here, we consider the contributions of SST, SAT, SH, SLP and the wind field to rapid decline of autumn sea ice.

Temperatures over the Arctic Ocean can influence Arctic sea ice directly through positive ice–temperature (SST or SAT) feedbacks. Changes in temperature also lead to changes in SH, SLP and wind, influencing Arctic sea ice through positive feedbacks between ice and SLP, wind or SH.

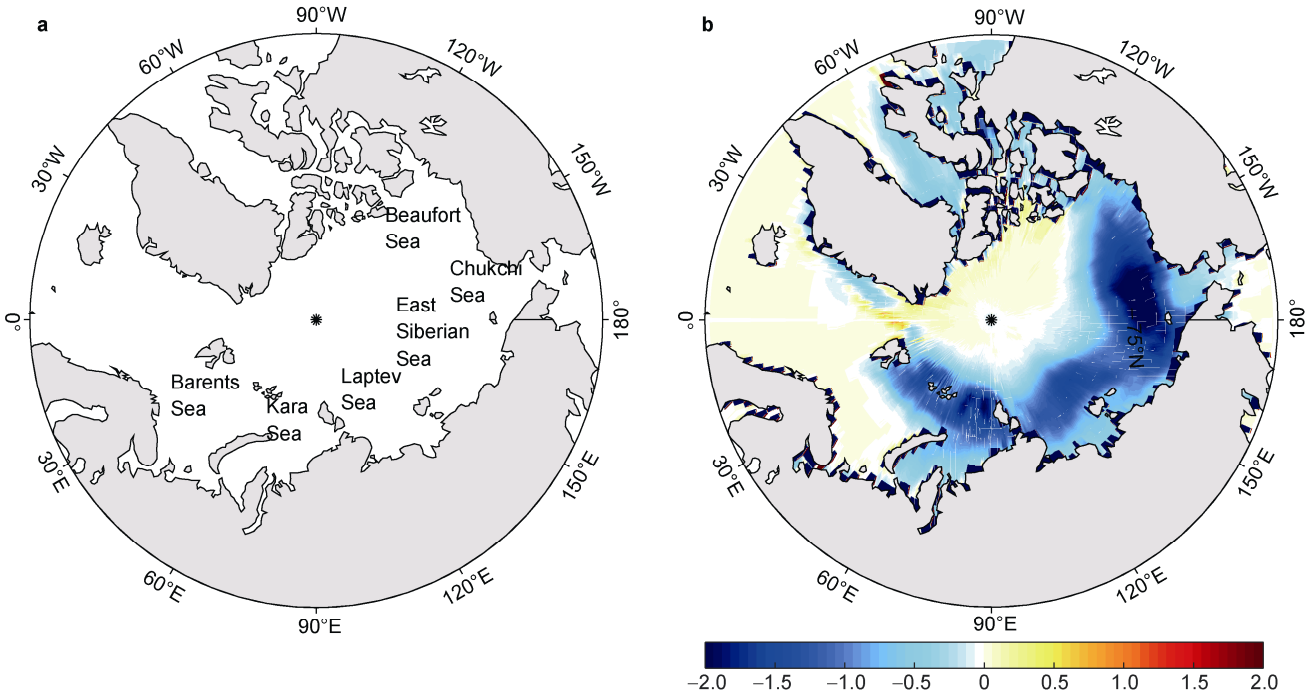

Figure 1 **a**, A map of the Arctic with major sea areas labeled; **b**, Arctic sea ice concentration anomalies for September, October and November (Sep–Nov) 2020 relative to Sep–Nov 1982. Gray shading indicates land.

We calculated the correlation coefficients between autumn SIE anomalies and the anomalies of SST, SAT and SH, respectively (Table 1). The correlation coefficients were calculated for three periods: July to September (Jul–Sep), August to October (Aug–Oct) and September to November (Sep–Nov). We use these broad and overlapping time periods to determine the periods with the highest coefficients for subsequent EOF analysis. Table 1 shows that SST, SAT and SH were all strongly negatively correlated with SIE. Absolute values of the Pearson correlation coefficients between the SIE anomalies and the SST and SAT anomalies were the largest in Aug–Oct. The absolute value of the correlation coefficient between autumn SIE anomalies and SH anomalies was the largest in Sep–Nov.

Table 1 Correlation coefficients between Arctic sea ice extent anomalies in autumn and sea surface temperature (SST), surface air temperature (SAT) and specific humidity (SH) anomalies

Months	Coefficients		
	SST	SAT	SH
Jul–Sep	−0.9207	−0.9347	−0.8540
Aug–Oct	−0.9410	−0.9446	−0.9259
Sep–Nov	−0.9371	−0.9240	−0.9436

We analyzed the time series of SIE anomalies in autumn, the SST and SAT anomalies in Aug–Oct and the SH anomalies in Sep–Nov (Figure 2). Arctic SIE decreased over the 39 years of the study period. The rate of decrease

was considerably higher after 2001. Linear regression analysis of SIE indicates that the rate of SIE decrease over 2002–2020 was almost twice that over 1982–2001. Years of low SIE mostly coincided with years of high SST, SAT and SH. Autumn SIE was at record low in 2007, 2012 and 2016. During these years, high SST, SAT and SH were recorded. The relationships shown in Figure 2 further corroborate the negative correlations presented in Table 1. However, the correlation coefficients and time series provide insufficient information to explain the relationships between SIE and SST, SAT and SH. Therefore, we conducted EOF analyses to better understand the factors and mechanisms contributing to the rapid decline of Arctic autumn sea ice over the past 39 years.

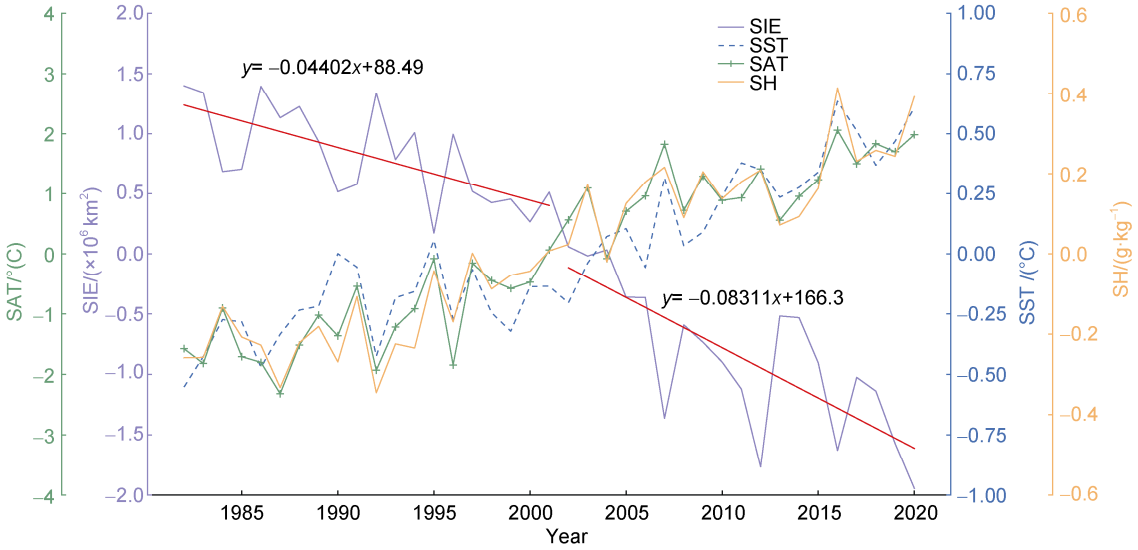

Figure 2 Average of Arctic SIE anomalies in autumn, SST anomalies in Aug–Oct, SAT anomalies in Aug–Oct, SH anomalies in Sep–Nov from 1982 to 2020. The sloping red lines in Figure 2 depict the SIE linear trends that fit over the time periods 1982–2001 and 2002–2020.

To further investigate the relationship between SST in Aug–Oct and Arctic sea ice in autumn, we conducted an EOF analysis of SST in the Arctic region. We focused on Aug–Oct because the correlation between SST and sea ice was the strongest during this period (Table 1). We examined the first EOF, which explains 39.07% of the total variance, and is the spatial pattern that explains the most variance of the data. The first EOF and the corresponding PC time series are shown in Figures 3a and 3d, respectively. In Figure 3a, positive values indicate SST increase while negative values indicate SST decrease. In areas covered by sea ice all year round, SST variation is zero. Between 1982 and 2020, SST increased in the Beaufort Sea, the East Siberian Sea, the Barents Sea, the Kara Sea and Laptev Sea where there was also a pronounced decrease of Arctic sea ice. Combining Figure 3a with Figure 3d, we found that SST mainly increased over the 39 years of the study period. The time coefficient changed from negative to positive around 2002, indicating that the mean SST over the entire study period was higher than the mean SST over the first part of the period prior to 2002 and was lower than the mean SST over the second part of the period after 2002. Small peaks in the time coefficient in 2007 and 2016 are consistent with the time series shown in Figure 2.

SST is an important indicator of sea ice feedback mechanisms. The first EOF of SST is mostly positive along the coast of the Arctic Ocean. Through the positive ice–SST feedback, SST leads to sea ice decrease along the coast, increasing the area of open water. Because the albedo of open water is much lower than that of sea ice, more sunlight is absorbed by the ocean surface, resulting in increase in absorption and decrease in reflection of solar radiation. As a result, the SST increases, heat is transferred to nearby sea ice that has remained intact, and leads to further melting of the ice. As the main variable of surface atmospheric circulation, SAT plays an important role in the melting and freezing of sea ice. We conducted an EOF analysis of SAT in the Arctic region in Aug–Oct between 1982 and 2020. The first EOF accounts for 63.54% for the total variance. The first EOF and the corresponding PC time series are shown in Figures 3b and 3d, respectively. In the Beaufort and East Siberian Seas, the first EOF is large and positive in Aug–Oct, and is consistent with the spatial distribution of SIE decline (Figure 1b). By combining Figure 3b with Figure 3d, we found that the SAT mainly increased over the study period. We also found a lag between SAT and SIE, similar to that between SST and SIE. Temperature increases prior to and including month X were associated with sea ice decline in month X, while sea ice decline in month X was also associated with temperature increase in month $X+1$, indicating the presence of a positive ice–SAT feedback mechanism. As the main variable of surface atmospheric circulation, SAT has a direct impact on the melting of sea ice. It also affects the SLP, the wind field and the SH, which in turn influence the melting of sea ice. Upwelling longwave radiation is a component of the sea surface heat

budget. It is a function of sea surface water temperature, atmospheric water vapor content and other variables. SH is the ratio of water vapor mass to total moist air mass. It also plays an important role in the melting of sea ice. As SAT increased, regions with relatively high SH (Figure 3c) also experienced relatively large decreases in SIC. When the moisture content in the air is high, relative humidity increases even if the temperature remains unchanged. The outgoing long-wave radiation from surface to outer space increases, and the significant reradiation of the sea surface decreases, resulting in the increase of SAT and SST (Cui et al., 2015). Therefore, SH also has an indirect effect on sea ice through its influence on temperature. As sea ice melts, it releases water vapor into the atmosphere. As open water area increases, evaporation increases, which further increases the water vapor content in the air, reinforcing the relationship between SH increase and SIC reduction. The first EOF of SH and the corresponding time coefficient are shown in Figures 3c and 3d, respectively. The first EOF explains 47.60% of the total variance, and is positive over the main regions of sea ice decline. It is large and positive in autumn in the Chukchi Sea, the East Siberian Sea, the Kara Sea and the Barents Sea. The corresponding time coefficient shows that SH mainly increased over the 39 years of the study period (Figure 3d). The corresponding time coefficients of SST, SAT and SH show roughly the same pattern. They changed from negative to positive around 2002. In particular, mean SST, SAT and SH over the last 18 years of the study period were higher than mean SST, SAT and SH over the entire study period.

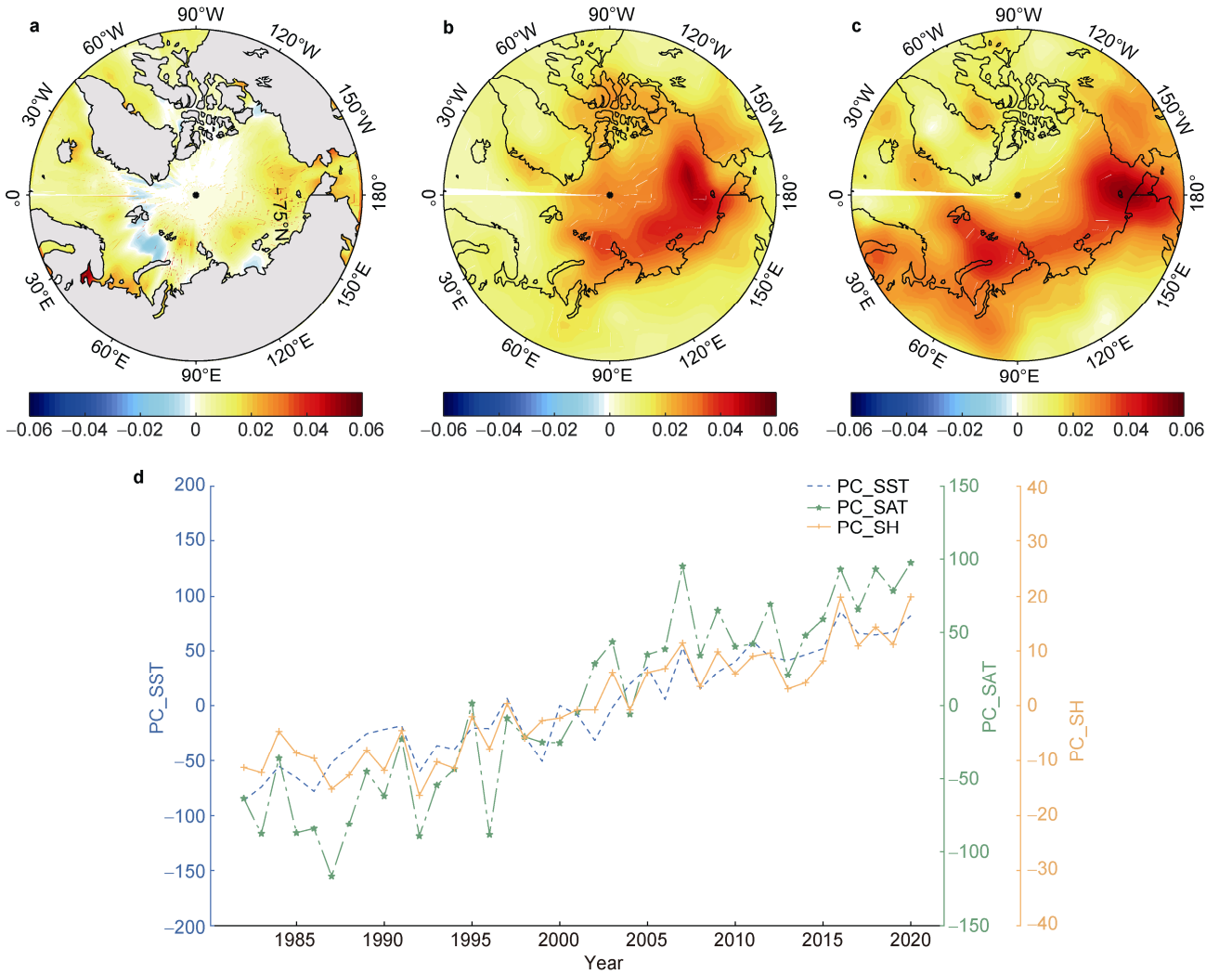

Figure 3 The first EOFs of (**a**) SST in August, September and October (Aug–Oct), (**b**) SAT in August, September and October (Aug–Oct), (**c**) SH in September, October and November (Sep–Nov), and (**d**) the corresponding PC time series of SST, SAT and SH. All analyses were conducted for 1982–2020. Gray shading indicates land.

In addition, SLP and the wind field also play important roles in the melting of Arctic sea ice. Therefore, we conducted an EOF analysis of SLP and the wind field in Aug–Oct. The first EOF of SLP accounts for 41.57% of the total variance. The first EOFs of zonal wind and meridional wind account for 25.22% and 30.96% of the total variance,

respectively. The first EOFs of the SLP, zonal wind and meridional wind in the Arctic region in Aug–Oct between 1982 and 2020 and their corresponding PC time series are shown in Figure 4.

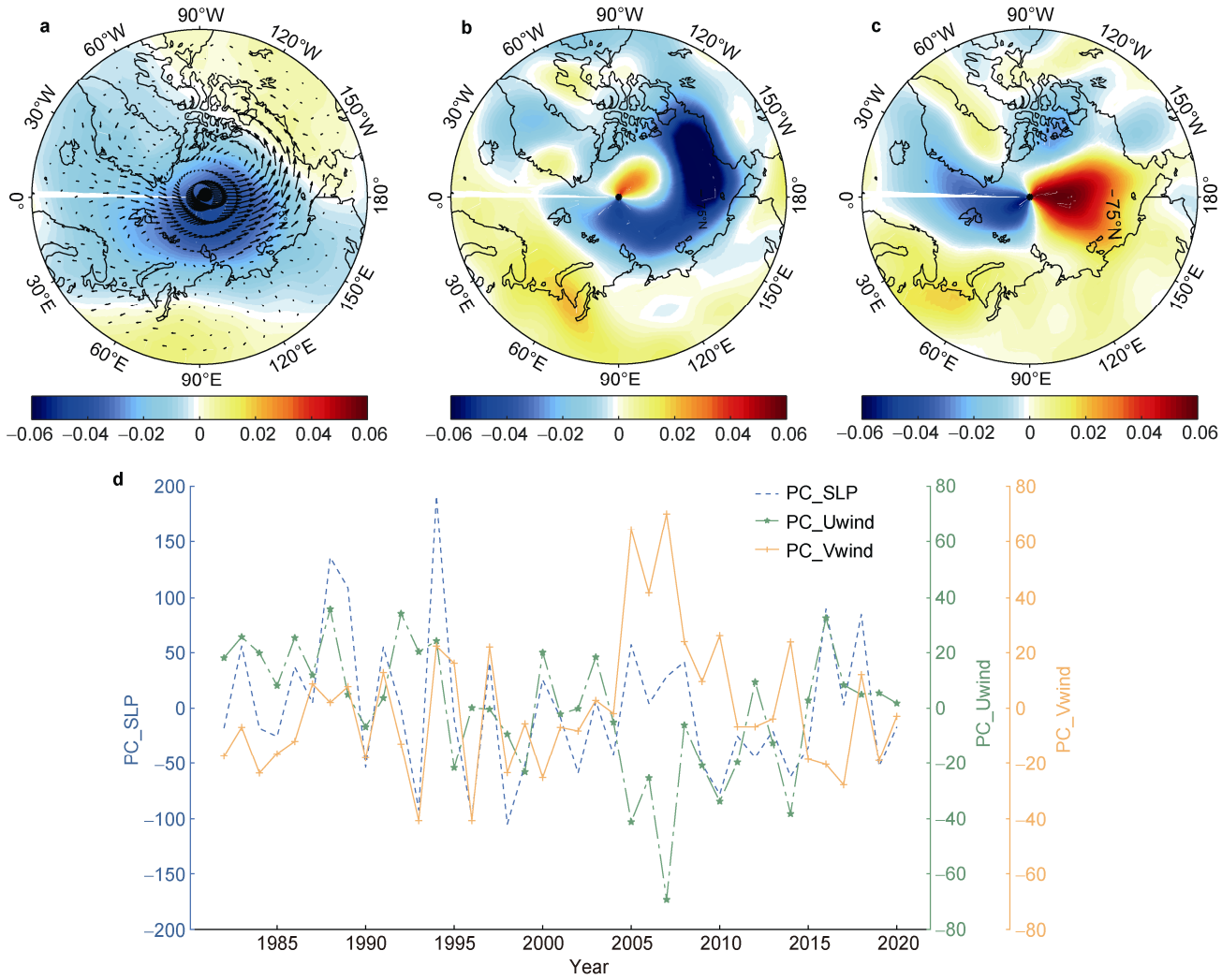

Figure 4 The first EOFs of (**a**) SLP, (**b**) zonal wind, (**c**) meridional wind in the Arctic in August, September and October (Aug–Oct), and (**d**) the corresponding PC time series. All analyses were conducted for 1982–2020.

The first EOF of SLP in Aug–Oct indicates the presence of a low pressure pattern over the Arctic (Figure 4a), with surface winds blowing from the Norwegian Sea and the Greenland Sea to the Arctic Ocean. We compared the first EOF of SLP with SIC decline and found that SLP decreased in areas of SIC decline. The first EOFs of SST and SH are strongly positive over the North Atlantic. The low pressure pattern over the Arctic brought warm seawater and moist air from the North Atlantic to the Arctic, causing considerable decrease in sea ice.

We analyzed the first EOFs of zonal wind and meridional wind. The EOF of zonal wind exhibits a relatively uniform distribution over the Arctic Ocean, and variability is the largest around the North Pacific Ocean. It is mainly negative over the Laptev Sea, the East Siberian Sea, the Chukchi Sea and the Beaufort Sea in Aug–Oct, and is positive over Europe, most of Russia and the North Atlantic. The EOF of meridional wind in Aug–Oct exhibits two distinct patterns. It is negative from the North Atlantic to the North Pole, and positive from the North Pacific to the North Pole. We compared the wind field with SIC, and found that enhancement of meridional wind and weakening of zonal wind resulted in warm air blowing from high pressure to low pressure areas and towards the polar region. Over the Chukchi Sea, the strengthening of meridional wind and weakening of zonal wind cause heat to flow in from the Pacific Ocean. SST increases and the freezing rate decreases during the early stages of freezing. Sea ice decline in the East Siberian Sea, the Beaufort Sea, the Laptev Sea and the Kara Sea is accelerated, forming feedback mechanisms between sea ice and SLP and the wind field.

Figure 5 summarizes the positive and negative ice–SST, ice–SAT, ice–SH and ice–SLP feedback mechanisms that we have examined and verified through

EOF analyses of SST, SAT, SH, SLP and the wind field. Temperatures can influence the melting of sea ice, creating ice–temperature (SST or SAT) feedbacks. Temperature increase leads to the melting of sea ice, which increases the area of open water and leads to further melting of sea ice. The decrease in albedo and increase in the absorption of shortwave radiation lead to cloud formation or atmospheric warming. This further increases downward and upward longwave radiation. Changes in temperature and sea level lead to changes in ocean currents, which influence atmospheric circulation through air–sea interactions, and in turn, impact sea ice. As temperature rises, evaporation increases, leading to an increase in the amount of water vapor in the atmosphere. With more water vapor, the atmosphere absorbs more longwave radiation, leading to temperature increase and acceleration of the melting of sea ice, thus, creating a positive ice–SH feedback. When the SLP decreases, the cyclonic circulation pattern formed by the low pressure center over the Arctic results in the weakening of the zonal wind and strengthening of the meridional wind. This counterclockwise circulation brings warm and moist air from the lower latitudes into the Arctic, accelerating the melting of sea ice and forming a positive ice–SLP feedback.

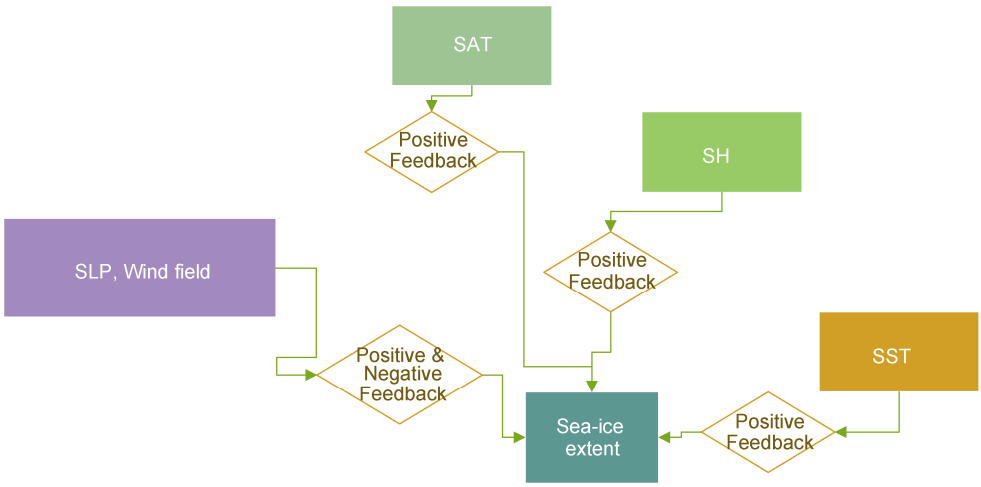

Figure 5 The feedback mechanisms of SST, SAT, SH, SLP and wind field with sea ice.

4 Conclusions and discussion

We investigated the decline of Arctic sea ice between 1982 and 2020 using NOAA OI SST V2 data. In terms of the spatial distribution of sea ice decline, linear regression analysis indicates a negative trend in SIC in most parts of the Arctic Ocean. Sea ice has been clearly declining in the Beaufort and Barents seas, and the rates of decline were the highest in the Beaufort Sea. The correlation coefficients between SIE anomalies and anomalies of SST, SAT and SH were calculated for different periods (Table 1). Results show negative correlations between sea ice and the other variables. The absolute values of the correlation coefficients are highest for Aug–Oct. Therefore, to identify the factors contributing to sea ice decline, we focused our analysis on these months, and examined the time series of the different variables. We found that the SIE decreased in Sep–Nov, SST and SAT clearly increased in Aug–Oct, and the SH clearly increased in Sep–Nov.

Furthermore, we conducted EOF analyses of SLP, the wind field and other variables for the same months. The first EOFs of SST, SAT and SH account for 39.07%, 63.54%, 47.60% of the total variances, respectively. Positive values are mainly concentrated between the Beaufort and Barents Seas. The PC time series indicate positive trends. These results verify the existence of the positive ice–SST, ice–SAT and ice–SH feedbacks in the Arctic. These feedback mechanisms contribute to the rapid sea ice decline observed in different months. The first EOFs of SLP, zonal wind and meridional wind explain 41.57%, 25.22%, 30.96% of the total variances, respectively. A low pressure center over the Arctic Ocean results in the weakening of the zonal wind over the Beaufort, Chukchi and East Siberian seas, reducing the resistance to warm winds blowing from the lower latitudes. The meridional wind also strengthens in these areas, verifying the ice–SLP feedback mechanism in the Arctic. The combined effects of these feedback mechanisms contribute to the rapid melting of autumn sea ice in the Arctic.

We conclude that increases in SST, SAT and SH, as well as changes in SLP and near-surface winds all impact the melting of sea ice. In this study, we examined four feedback mechanisms. Other factors also affect the melting of sea ice. These include the polar vortex in the troposphere (Overland and Wang, 2016; Savelieva, 2020), sea ice age and ice thickness (Spreen et al., 2011; Serreze and Meier, 2019). These factors also have impacts on climatic changes (Kim et al., 2013) and need to be investigated further. Our analysis was based on observational data. Future studies can also include numerical atmospheric models to further investigate the relationships between sea ice and different variables.

Acknowledgments We thank all the collaborators of this project. We also thank our colleagues who contributed to drafting the manuscript. NOAA_OI_SST_V2 data provided by the NOAA/OAR/ESRL PSL, Boulder, Colorado, USA, from their Web site at https://psl.noaa.gov/data/gridded/data.noaa.oisst.v2.html. NCEP Reanalysis Derived data provided by the NOAA/OAR/ESRL PSL, Boulder, Colorado, USA, from their Web site at https://www.psl.noaa.gov/data/gridded/data.ncep.reanalysis.derived.pressure.html. This work was supported by the Marine S&T Fund of Shandong Province for Pilot National Laboratory for Marine Science and Technology (Qingdao) (Grant no. 2018SDKJ0106-1), Open Fund of the Key Laboratory of Ocean Circulation and Waves, Chinese Academy of Sciences (Grant no. KLOCW2003), and the Project of Doctoral Found of Qingdao University of Science and Technology (Grant no. 2100100 22746). We appreciate two anonymous reviewers and Associate Editor, Dr. Ian Allison for their valuable suggestions and comments regarding further improvement of this article.

References

Ballinger T J, Overland J E, Wang M et al. 2020. Arctic report card 2020: surface air temperature.

Belchansky G I, Douglas D C, Platonov N G. 2004. Duration of the Arctic sea ice melt season: regional and interannual variability, 1979–2001. J Climate, 17(1): 67-80, doi:10.1175/1520-0442(2004)017<0067: dotasi>2.0.co;2.

Cohen J, Screen J A, Furtado J C, et al. 2014. Recent Arctic amplification and extreme mid-latitude weather. Nat Geosci, 7(9): 627-637, doi:10.1038/ngeo2234.

Comiso J C, Parkinson C L, Gersten R, et al. 2008. Accelerated decline in the Arctic sea ice cover. Geophys Res Lett, 35(1): L01703, doi:10.1029/2007GL031972.

Cui H Y, Qiao F L, Shu Q, et al. 2015. Causes for different spatial distributions of minimum Arctic sea-ice extent in 2007 and 2012. Acta Oceanol Sin, 34(9): 94-101, doi:10.1007/s13131-015-0676-x.

Ding Q H, Schweiger A, L'Heureux M, et al. 2017. Influence of high-latitude atmospheric circulation changes on summertime Arctic sea ice. Nat Clim Change, 7(4): 289-295, doi:10.1038/nclimate3241.

Fetterer F, Knowles K, Meier W N, et al. 2017. NOAA/NSIDC climate data record of passive microwave sea ice concentration, version 3. NSIDC: National Snow and Ice Data Center, Boulder, Colorado, USA.

Goosse H, Gerdes R, Kauker F, et al. 2004. Influence of the exchanges between the Atlantic and the Arctic on sea ice volume variations during the period 1955–97. J Climate, 17(6): 1294-1305, doi:10.1175/1520-0442(2004)017<1294: iotebt>2.0.co;2.

Gui D W, Pang X P, Lei R B, et al. 2019. Changes in sea ice kinematics in the Arctic outflow region and their associations with Arctic Northeast Passage accessibility. Acta Oceanol Sin, 38(8): 101-110, doi:10.1007/s13131-019-1451-1.

Huang Y Y, Dong X Q, Bailey D A, et al. 2019. Thicker clouds and accelerated arctic sea ice decline: the atmosphere–sea ice interactions in spring. Geophys Res Lett, 46(12): 6980-6989, doi:10.1029/2019GL082791.

Kim S J, Choi H S, Kim B M, et al. 2013. Analysis of recent climate change over the Arctic using ERA-Interim reanalysis data. Adv Polar Sci, 24(4): 326-338, doi:10.3724/sp.j.1085.2013.00326.

Letterly A, Key J, Liu Y H. 2016. The influence of winter cloud on summer sea ice in the Arctic, 1983–2013. J Geophys Res: Atmos, 121(5): 2178-2187, doi:10.1002/2015JD024316.

Liang Y, Bi H B, Wang Y H, et al. 2020. Role of atmospheric factors in forcing Arctic sea ice variability. Acta Oceanol Sin, 39(9): 60-72, doi:10.1007/s13131-020-1629-6.

Lind S, Ingvaldsen R B, Furevik T. 2018. Arctic warming hotspot in the northern Barents Sea linked to declining sea-ice import. Nat Clim Change, 8(7): 634-639, doi:10.1038/s41558-018-0205-y.

Ma L P, Woollings T, Williams R G, et al. 2020. How does the winter jet stream affect surface temperature, heat flux, and sea ice in the North Atlantic? J Clim, 33(9): 3711-3730, doi:10.1175/jcli-d-19-0247.1.

Markus T, Stroeve J C, Miller J. 2009. Recent changes in Arctic sea ice melt onset, freezeup, and melt season length. J Geophys Res: Oceans, 114(C12): C12024, doi:10.1029/2009JC005436.

Nakamura T, Yamazaki K, Iwamoto K, et al. 2015. A negative phase shift of the winter AO/NAO due to the recent Arctic sea-ice reduction in late autumn. J Geophys Res: Atmos, 120(8): 3209-3227, doi:10.1002/2014JD022848.

Ogi M, Rigor I G. 2013. Trends in Arctic sea ice and the role of atmospheric circulation. Atmos Sci Lett, 14(2): 97-101, doi:10.1002/asl2.423.

Ogi M, Rigor I G, McPhee M G, et al. 2008. Summer retreat of Arctic sea ice: Role of summer winds. Geophys Res Lett, 35(24): L24701, doi:10.1029/2008GL035672.

Ogi M, Rysgaard S, Barber D G. 2016. Importance of combined winter and summer Arctic Oscillation (AO) on September sea ice extent. Environ Res Lett, 11(3): 034019, doi:10.1088/1748-9326/11/3/034019.

Ogi M, Wallace J M. 2007. Summer minimum Arctic sea ice extent and the associated summer atmospheric circulation. Geophys Res Lett, 34(12): L12705, doi:10.1029/2007GL029897.

Overland J E, Wang M Y. 2016. Recent extreme Arctic temperatures are due to a split polar vortex. J Clim, 29(15): 5609-5616, doi:10.1175/jcli-d-16-0320.1.

Perovich D, Meier W, Tschudi M, et al. 2020. Arctic report card 2020: sea ice.

Platov G, Iakshina D, Krupchatnikov V. 2020. Characteristics of atmospheric circulation associated with variability of sea ice in the Arctic. Geosciences, 10(9): 359, doi:10.3390/geosciences10090359.

Rigor I G, Wallace J M, Colony R L. 2002. Response of sea ice to the Arctic oscillation. J Climate, 15(18): 2648-2663, doi:10.1175/1520-0442(2002)015<2648: rositt>2.0.co;2.

Savelieva E. 2020. Possible influence of the tropospheric polar vortex on the Barents Sea ice extent in winter. J Atmos Sol Terr Phys, 197: 105173, doi:10.1016/j.jastp.2019.105173.

Schweiger A J, Lindsay R W, Vavrus S, et al. 2008. Relationships between Arctic sea ice and clouds during autumn. J Clim, 21(18): 4799-4810, doi:10.1175/2008jcli2156.1.

Serreze M C, Meier W N. 2019. The Arctic's sea ice cover: trends, variability, predictability, and comparisons to the Antarctic. Ann NY Acad Sci, 1436(1): 36-53. doi:10.1111/nyas.13856.

Serreze M C, Stroeve J. 2015. Arctic sea ice trends, variability and implications for seasonal ice forecasting. Philos T R Soc A, 373(2045): 20140159. doi:10.1098/rsta.2014.0159.

Spreen G, Kwok R, Menemenlis D. 2011. Trends in Arctic sea ice drift and role of wind forcing: 1992–2009. Geophys Res Lett, 38(19): L19501,

doi:10.1029/2011GL048970.

Stroeve J C, Markus T, Boisvert L, et al. 2014. Changes in Arctic melt season and implications for sea ice loss. Geophys Res Lett, 41(4): 1216-1225, doi:10.1002/2013GL058951.

Thompson D W J, Wallace J M. 1998. The Arctic oscillation signature in the wintertime geopotential height and temperature fields. Geophys Res Lett, 25(9): 1297-1300, doi:10.1029/98GL00950.

Timmermans M L, Labe Z. 2020. Arctic report card 2020: sea surface temperature.

Urrego-Blanco J R, Hunke E C, Urban N. 2019. Emergent relationships among sea ice, longwave radiation, and the Beaufort high circulation exposed through parameter uncertainty analysis. J Geophys Res: Oceans, 124(12): 9572-9589, doi:10.1029/2019JC014979.

Wu B Y, Overland J E, D'Arrigo R. 2012. Anomalous Arctic surface wind patterns and their impacts on September sea ice minima and trend. Tellus A: Dyn Meteorol Oceanogr, 64(1): 18590, doi:10.3402/tellusa.v64i0.18590.

Yang X Y, Yuan X, Ting M. 2016. Dynamical link between the Barents–Kara sea ice and the Arctic oscillation. J Clim, 29(14): 5103-5122.

Zhang S Y, Gan T Y, Bush A B G. 2020. Variability of Arctic sea ice based on quantile regression and the teleconnection with large-scale climate patterns. J Clim, 33(10): 4009-4025, doi:10.1175/jcli-d-19-0375.1.